JACS
JOURNAL OF THE AMERICAN CHEMICAL SOCIETY
Communication
pubs.acs.org/JACS

Macroscale Lateral Alignment of Semiconductor Nanorods into Freestanding Thin Films

Tie Wang,[†] Xirui Wang,[†] Derek LaMontagne,[†] Zhongwu Wang,[‡] and Y. Charles Cao*[,†]

[†]Department of Chemistry, University of Florida, Gainesville, Florida 32611, United States
[‡]Cornell High Energy Synchrotron Source (CHESS), Wilson Laboratory, Cornell University, Ithaca, New York 14853, United States

Supporting Information

ABSTRACT: This Communication reports that needle-like supercrystalline colloidal particles can be synthesized through anisotropy-driven self-assembly of 1,12-dodecanediamine-functionalized CdSe/CdS core/shell nanorods. The resulting superparticles exhibit both 1D lamellar and 2D hexagonal supercrystalline orders along directions parallel and perpendicular to the long axis of constituent nanorods, respectively. Our results show that the needle-like superparticles can be unidirectionally aligned through capillary forces on a patterned solid surface and further transferred into macroscopic, uniform, freestanding polymer films, which exhibit strong linear polarized PL with an enhanced polarization ratio, and are useful as energy down-conversion phosphors in polarized LEDs.

Self-assembly, driven by non-covalent interactions (e.g., van der Waals, dipolar, entropic force, etc.), is the fundamental mechanism behind the formation of cellular machineries that perform essential functions of life.[1] It has been found that interaction anisotropy dictates the structural complexity and functional specificity of naturally occurring cellular machines.[1a,b,2] This finding stimulates research efforts based on anisotropy to design and control the self-assembly of nanoparticles into well-defined 2D and 3D complex structures, which may provide a low-cost, programmable paradigm to synthesize functional solid-state materials that are not easily accessible via conventional methods.[3] For example, these materials can exhibit properties inherited from their individual nanoparticle constituents as well as collective properties induced from the coupling effects between their constituents.[4] In the current literature, the discovered collective properties of nanoparticle superlattices include spin-dependent electron transport, vibrational coherence, enhanced conductivity, tandem catalysis, reversible metal-to-insulator transitions, enhanced ferro- and ferrimagnetism, tunable magneto-transport, and efficient charge transport.[5]

To date, anisotropic nanoparticles have been used in the design of directional bonding interactions on the nanometer scale through crystal-face-specific functionalization of these particles with recognition groups and/or through shape-induced anisotropic interactions.[6] Recently, we have reported that anisotropy-driven self-assembly of CdSe/CdS semiconductor core/shell nanorods can produce 3D colloidal superparticles with multiple well-defined supercrystalline domains under thermodynamic control, or yield needle-like superparticles with a single supercrystalline domain through a kinetic process.[7] This kinetic process is dictated by kinetically induced anisotropic and crystal-face-specific functionality of the nanorods, wherein their bottom and top faces exhibit greater solvophobicity than their side faces.[7] However, in this process, the formation of needle-like superparticles is sensitively dependent on the level of octylamine ligands on the surface of CdSe/CdS nanorods, which requires a surface treatment for incubating CdSe/CdS nanorods in a very dilute octylamine/chloroform (0.1%, v/v) solution for 6−7 days.[7] This requirement makes it very inconvenient to use this kinetic approach for making needle-like superparticles.

To overcome this difficulty, here we report a new synthesis for making needle-like CdSe/CdS supercrystals, which is based on the preparation of CdSe/CdS nanorods exhibiting a static structure with hydrophobic anisotropy through surface functionalization with 1,12-dodecanediamine. Because 1,12-dodecanediamine ligands are primarily functionalized onto the side faces of CdSe/CdS nanorods, their bottom and top faces exhibit more hydrophobicity than their side faces due to the hydrophilicity of amine groups. Therefore, the hydrophobic anisotropy of the resultant nanorods leads to the formation of needle-like superparticles through a process of self-assembly of these nanorods. Significantly, the surface treatment of 1,12-dodecanediamine requires only 10 min, and the quality of the resulting needle-like superparticles is comparable to that of those made using octylamine treatment for 6−7 days. In addition, because the 1,12-dodecanediamine functionalized nanorods exhibit a static hydrophobicity-anisotropic structure, the synthesis here can yield needle-like superparticles with diameters of $(2.00 \pm 0.43) \times 100$ nm, which is about 5 times narrower than those needle-like superparticles $(1.1 \pm 0.3) \times 1000$ nm made using the octylamine treatment. These narrower superparticles are important in their applications as energy down-conversion light-emitting diodes (LEDs) because a narrower size can minimize the light loss caused by Rayleigh scattering, which is important for their use as energy down-conversion phosphors in manufacturing polarized LEDs.

In this study, colloidal CdSe/CdS superparticles were prepared using a previously developed approach, in which superparticles are made through controlled induction of solvophobic interactions (CIS).[7,8] The CIS approach includes two major steps: (i) synthesis of water-soluble nanorod micelles; and (ii) growth of superparticles from nanorod micelles in an aqueous solution of ethylene glycol. We synthesized highly fluorescent CdSe/CdS nanorods (77 ± 2.1 nm in length and 4.5

Received: March 11, 2013
Published: April 12, 2013

dx.doi.org/10.1021/ja402539f | J. Am. Chem. Soc. 2013, 135, 6022−6025

Scheme 1. Formation of (a) Needle-like[a] and (b) a Double-Domed Cylinder[b] Superparticles from CdSe/CdS Nanorods: (i) Nanorod Micelle and (ii) Superparticle Formation

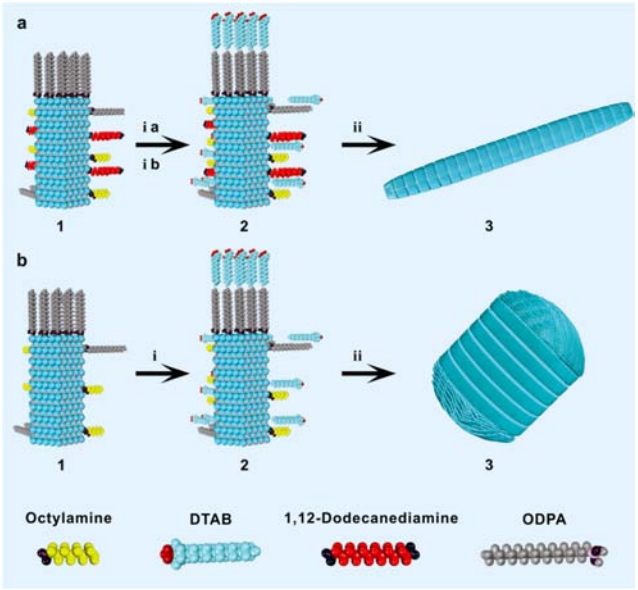

[a]Proposed model for the process of forming needle-like superparticles: (a1) a CdSe/CdS nanorod functionalized with ODPA, 1,12-dodecanediamine, and octylamine, (a2) a nanorod micelle prepared using DTAB, and (a3) a needle-like superparticle. [b]Proposed model for the progress of forming DDC superparticles: (b1) a CdSe/CdS nanorod functionalized with ODPA and octylamine, (b2) a nanorod micelle prepared using DTAB, and (b3) a DDC superparticle.

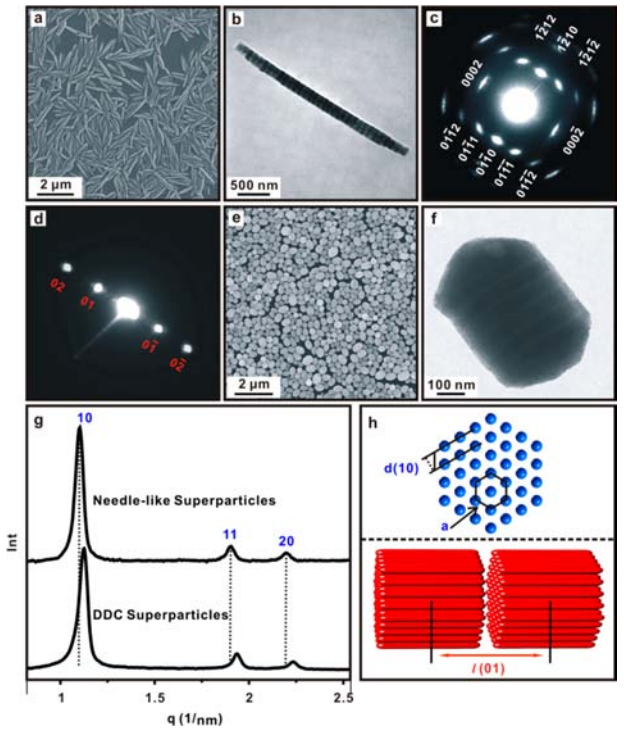

Figure 1. (a) SEM and (b) TEM images of needle-like superparticles. (c) Wide-angle and (d) small-angle ED patterns of needle-like superparticles shown in (b). (e) SEM and (f) TEM images of DDC superparticles. (g) Integrated data of the SAXS pattern of needle-like (top) and DDC (bottom) superparticles. (h) Model for the 2D hexagonally packed structure (top, in blue) and 1D lamellar structure (bottom, in red). $q = (4\pi/\lambda)\sin\theta$.

± 0.3 nm in diameter, see Figure S1) primarily capped with octylamine and octadecylphosphonic acid (ODPA) according to a literature method,[9] functionalized the nanorods with 1,12-dodecanediamine, and used them to prepare nanorod micelles (*vide infra*). Because the surface of CdSe/CdS nanorods exhibit atomic packing factor anisotropy, their bottom and top {0001} faces have a higher ligand packing density than their side faces, such as $\{10\bar{1}0\}$ and $\{11\bar{2}0\}$ (Figure S2).[7] This ligand-packing density anisotropy allows for the preferential attachment of 1,12-dodecanediamine onto the side faces of CdSe/CdS nanorods under appropriate conditions, thus resulting in the solvophobicity anisotropy of the resulting nanorods, whose side faces are less hydrophobic (or solvophobic herein) than their bottom and top faces (Scheme 1).

In a typical superparticle synthesis, 1,12-dodecanediamine (0.2 μL) was mixed with a chloroform solution containing CdSe/CdS nanorods (10 mg/mL, 1 mL), and the mixture solution was stirred for 10 min. Then the resulting nanorod solution was mixed with a dodecyltrimethylammonium bromide (DTAB) solution (20 mg/mL, 1 mL) using a vortex mixer. A clear, yellow nanorod-micelle aqueous solution was obtained by evaporating chloroform from the mixture solution via bubbling Ar at 40 °C. Under vigorous stirring, the nanorod-micelle aqueous solution was injected into a three-neck flask with ethylene glycol (5.0 mL), causing the decomposition of nanorod micelles due to the loss of DTAB molecules into the growth solution, which, in turn, induce solvophobic interactions between the nanorod surfaces and solvent molecules (i.e., water and ethylene glycol). This process leads to the aggregation of nanorods, ormation of superparticle embryos in the aqueous ethylene glycol solution, and subsequent formation of superparticles through the colloidal crystallization of nanorods inside the embryos (Figure S3). After 10 min of stirring, an aqueous solution of dithiol-functionalized Tween-20 (0.1 mM, 1.0 mL, see Supporting Information) was added into the growth solution to stabilize the superparticles.[7,8c] The resulting superparticles were isolated and purified twice by centrifugation (3300 rpm, 5 min). As-prepared superparticles are highly dispersible in polar solvents, and indefinitely stable in solvents with strong polarity such as water and ethanol.

Low-magnification scanning electron microscopy (SEM, Figure 1a) shows that the resulting superparticles exhibit a needle-like shape with a diameter of (2.00 ± 0.43) × 100 nm and a length of (1.30 ± 0.49) × 1000 nm. A higher magnification transmission electron microscopy (TEM, Figure 1b) image show that a typical needle-like superparticle has a lamellar structure that comprises stacked multilayer discs formed from closely packed nanorods lying parallel to the superparticle long axis. The TEM observation is consistent with selected-area electron diffraction (SAED) measurements, which also provide structural information of nanorod packing inside the superparticle. A wide-angle SAED pattern (Figure 1c) of the needle-like superparticle is composed of a set of strong $[10\bar{1}0]$-zone diffraction dots and a set of weak $[21\bar{1}0]$-zone dots. This SAED pattern indicates that although the alignment of nanorods in the superparticle is not perfect at the atomic level (largely due to the rotational freedom around their long axes), the long axes of the nanorod constituents are parallel to each other as well as to the long axis of the superparticle.[7,8c] In addition, the small-angle SAED measurements show that the superparticle exhibits a 1D lamellar structure with a lattice constant (l) of 80.2 nm, which, together with the value of nanorod length measured using TEM,

dx.doi.org/10.1021/ja402539f | J. Am. Chem. Soc. 2013, 135, 6022−6025

determines that the end-to-end distance between neighboring constituent nanorods is 3.2 nm (Figure 1d,h).

The supercrystalline structure of needle-like superparticles was further characterized using synchrotron-based small-angle X-ray scattering (SAXS, Figure 1g). The peaks in the SAXS pattern can be indexed into the (10), (11), and (20) Bragg diffractions of a hexagonal lattice with a unit cell constant (a) of 6.7 ± 0.1 nm (Figure 1g,h). This datum, together with the value of rod diameter determined from TEM observation, suggests that the side-by-side distance of neighboring rods is 2.2 ± 0.5 nm. This distance is substantially shorter than twice the length of an ODPA ligand (~3.4 nm),[10] suggesting that the long chains of ODPA ligands are intercalated between neighboring nanorods at the side faces of the nanorods. The side-by-side interparticle distance (2.2 ± 0.5 nm) is shorter than the end-to-end distance (3.2 nm), which is consistent with the anisotropic surface functionalization of the nanorods (*vide supra*).

The formation of needle-like supercrystalline particles is in agreement with the solvophobicity anisotropy of the 1,12-dodecanediamine-functionalized CdSe/CdS nanorods, whose side faces are less solvophobic than their bottom and top faces (Scheme 1).[7] In solution, the solvophobicity anisotropy of the nanorods leads to the anisotropy of the specific Gibbs free energy of their faces: their bottom and top faces exhibit a higher specific Gibbs free energy than their side faces.[1d] Thus, during the synthesis of supercrystalline particles, minimizing the Gibbs free energy of maturing superparticles leads to rapid growth of supercrystalline domains along the long axes of constituent nanorods during colloidal crystallization, which forms needle-like superparticles.[7]

In contrast, a control experiment using CdSe/CdS nanorods treated with an identical amount of octylamine for an identical treatment time formed superparticles with a morphology of double-domed cylinders (DDCs) with a diameter of (3.50 ± 0.63) × 100 nm and a length of (4.30 ± 0.76) × 100 nm, whose formation has been identified to be the consequence of minimizing the Gibbs free energy of maturing superparticles made from CdSe/CdS nanorods without solvophobicity anisotropy.[7] The SAXS pattern of these DDC superparticles shows that they exhibit a hexagonal superlattice with a unit cell constant of 6.5 ± 0.1 nm (Figure 1g,h), suggesting that the side-by-side distance of neighboring rods in DDC superparticles is 2.0 ± 0.5 nm, slightly shorter than in the needle-like superparticles (2.2 ± 0.5 nm), indicating that the presence of 1,12-dodecanediamine slightly increases the interparticle distance in the needle-like superparticles (Figure 1g,h). Another control experiment using CdSe/CdS nanorods treated with dodecylamine in an identical procedure again only yielded DDC superparticles (Figure S5), which further confirms the importance of 1,12-dodecanediamine treatment in the synthesis of needle-like superparticles. Note that the type of micelle-forming surfactant is important to the formation of superparticles. For example, when cetyltrimethylammonium bromide (CTAB) was used as the surfactant, no superparticle was formed because CTAB–nanorod micelles cannot be decomposed in ethylene glycol aqueous solutions under our experimental conditions.[8b]

Moreover, the resulting needle-like superparticles made from unoptimized synthesis exhibit a photoluminescence (PL) quantum yield of ~40%. These superparticles have a diffusion coefficient two or more orders of magnitude smaller than that of individual nanorods. Such a small diffusion coefficient substantially suppresses the Brownian-motion induced disordering

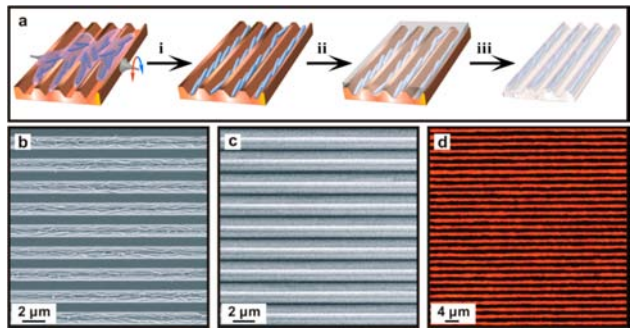

Figure 2. (a) Schematic illustration of process for the preparation of freestanding PDMS thin films embedded with unidirectionally aligned needle-like CdSe/CdS superparticles: (i) flow-assisted unidirectional alignment of needle-line CdSe/CdS superparticles, (ii) formation of PDMS film, and (iii) detachment of PDMS film from a template. (b) SEM image of laterally aligned needle-like superparticles on a Si_3N_4 pattern made via photolithography. (c) SEM and (d) optical fluorescence images of a PDMS thin film embedded with unidirectionally aligned needle-like superparticles.

and enables template-directed assembly of superparticles into macroscopic structures with microscopic uniformity.[11] In addition, because of their mesoscopic size, these needle-like superparticles are easily aligned into unidirectional line patterns on Si_3N_4 substrates through capillary forces (Figure 2).[12] The aligned superparticles can be readily transferred into uniform and removable thin films of polydimethylsiloxane (PDMS) with sizes of 2.5 cm × 5.0 cm (Figure 2a). Importantly, the resulting superparticle–PDMS composite thin films are highly transparent and exhibit strong linearly polarized PL at 600 nm with a typical emission polarization ratio $[\rho = (I_{\parallel} - I_{\perp})/(I_{\parallel} + I_{\perp})]$ of 0.89, where $I_{\parallel}$ and $I_{\perp}$ are the PL intensities parallel and perpendicular to the nanorod long axis, respectively (Figure 3). This ratio is substantially larger than the typical emission polarization ratio of individual single CdSe/CdS nanorods (0.75).[13] We attribute this PL anisotropy enhancement to a combination of two effects among the CdSe/CdS nanorods inside the elongated needle-like superparticles embedded in PDMS films: (1) dielectric effects and (2) collective electric-dipole coupling effects.[7,14]

Moreover, to demonstrate the usefulness of the superparticle-PDMS composite thin films (Figure 3), we built a light panel

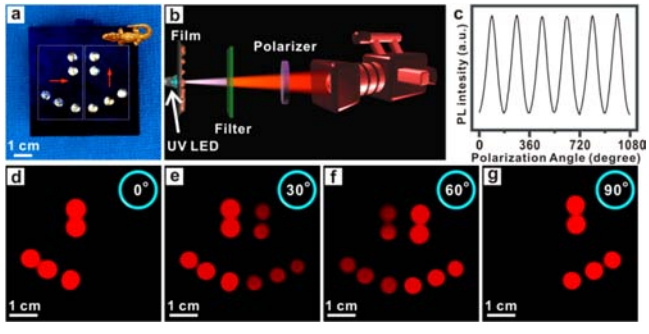

Figure 3. (a) Photograph of a light panel consisting of 10 LEDs, covered with two pieces of superparticle-embedded PDMS films. (b) Scheme for the measurements of polarized lights from the LED panel. (c) PL intensity as a function of polarization angle under an excitation wavelength of 380 nm. Optical images of a light panel as energy down-conversion phosphors taken with a polarizer at angles (d) 0°, (e) 30°, (f) 60°, and (g) 90°. The LEDs emit 600 nm red light with a bandwidth of 40 nm and a polarization ratio of ~0.89.

dx.doi.org/10.1021/ja402539f | J. Am. Chem. Soc. 2013, 135, 6022–6025

consisting of ten LEDs (λ = 380 nm, P = 20 mW, Super Bright LEDs, Inc., St. Louis, MO), which is covered with two pieces of superparticle−PDMS composite thin films with nanorod-alignment directions at a 90° angle. Under the backlighting of LEDs and through a 500-nm cutoff filter, the light panel showed orange emission dots, which can be seen by the naked eye (Figure 3d−g). Through a polarizer at different angles, the light panel displayed patterns of orange dots consistent with the nanorod-alignment directions in the two superparticle−PDMS composite thin films, which confirms that the thin films exhibit linearly polarized PL. All together, these results show that it is feasible to use superparticle−PDMS composite thin films as energy down-conversion phosphors to build polarized LEDs.

In conclusion, we report that needle-like supercrystalline colloidal particles can be synthesized through anisotropy-driven self-assembly of 1,12-dodecanediamine-functionalized CdSe/CdS core/shell nanorods. The resulting superparticles exhibit both 1D lamellar and 2D hexagonal supercrystalline orders along directions parallel and perpendicular to the long axis of constituent nanorods, respectively. In addition, the needle-like superparticles can be unidirectionally aligned through capillary forces on a patterned solid surface and further transferred into macroscopic, uniform, freestanding polymer films, which exhibit strong linearly polarized PL with an enhanced polarization ratio, and are useful as energy down-conversion phosphors in polarized LEDs. With further optimizations in the synthesis of core/shell nanorods with higher PL quantum yields and higher PL polarization ratios (e.g., high-quality CdSe/CdS rod-in-rod nanocrystals[13a]), we expect that the fluorescent superparticle-based polarized LEDs can potentially overcome the limit of 50% energy loss caused by conventional optical polarizers used in current liquid-crystal display devices,[15] which is important for applications such as large panel displays.

■ ASSOCIATED CONTENT

Ⓢ Supporting Information

Experimental details and additional data. This material is available free of charge via the Internet at http://pubs.acs.org.

■ AUTHOR INFORMATION

Corresponding Author

cao@chem.ufl.edu

Notes

The authors declare no competing financial interest.

■ ACKNOWLEDGMENTS

The authors acknowledge funding support from the Office of Naval Research (N00014-09-1-0441 and N00014-13-1-0325) and NSF (CHE-1213333). CHESS is supported by the NSF award DMR-0936384. TEM measurements were conducted at the Major Analytical Instrumentation Center at the University of Florida.

■ REFERENCES

(1) (a) Whitesides, G. M.; Grzybowski, B. *Science* **2002**, *295*, 2418. (b) Mann, S. *Nat. Mater.* **2009**, *8*, 781. (c) Glotzer, S. C.; Solomon, M. J. *Nat. Mater.* **2007**, *6*, 557. (d) Min, Y. J.; Akbulut, M.; Kristiansen, K.; Golan, Y.; Israelachvili, J. *Nat. Mater.* **2008**, *7*, 527.

(2) (a) Capito, R. M.; Azevedo, H. S.; Velichko, Y. S.; Mata, A.; Stupp, S. I. *Science* **2008**, *319*, 1812. (b) Gilroy, J. B.; Gadt, T.; Whittell, G. R.; Chabanne, L.; Mitchels, J. M.; Richardson, R. M.; Winnik, M. A.; Manners, I. *Nat. Chem.* **2010**, *2*, 566.

(3) (a) Korgel, B. A. *Nat. Mater.* **2010**, *9*, 701. (b) Quan, Z. W.; Fang, J. Y. *Nano Today* **2010**, *5*, 390. (c) Fan, H. Y.; Yang, K.; Boye, D. M.; Sigmon, T.; Malloy, K. J.; Xu, H. F.; Lopez, G. P.; Brinker, C. J. *Science* **2004**, *304*, 567. (d) Choi, J. J.; Bealing, C. R.; Bian, K. F.; Hughes, K. J.; Zhang, W. Y.; Smilgies, D. M.; Hennig, R. G.; Engstrom, J. R.; Hanrath, T. *J. Am. Chem. Soc.* **2011**, *133*, 3131. (e) Redl, F. X.; Cho, K. S.; Murray, C. B.; O'Brien, S. *Nature* **2003**, *423*, 968. (f) Caswell, K. K.; Wilson, J. N.; Bunz, U. H. F.; Murphy, C. J. *J. Am. Chem. Soc.* **2003**, *125*, 13914. (g) Song, C. Y.; Zhao, G. P.; Zhang, P. J.; Rosi, N. L. *J. Am. Chem. Soc.* **2010**, *132*, 14033. (h) Hickey, R. J.; Haynes, A. S.; Kikkawa, J. M.; Park, S. J. *J. Am. Chem. Soc.* **2011**, *133*, 1517. (i) Klajn, R.; Bishop, K. J. M.; Fialkowski, M.; Paszewski, M.; Campbell, C. J.; Gray, T. P.; Grzybowski, B. A. *Science* **2007**, *316*, 261.

(4) (a) Wang, T.; LaMontagne, D.; Lynch, J.; Zhuang, J.; Cao, Y. C. *Chem. Soc. Rev.* **2013**, *42*, 2804. (b) Kim, S. H.; Medeiros-Ribeiro, G.; Ohlberg, D. A. A.; Williams, R. S.; Heath, J. R. *J. Phys. Chem. B* **1999**, *103*, 10341. (c) Choi, C. L.; Alivisatos, A. P. *Annu. Rev. Phys. Chem.* **2010**, *61*, 369. (d) Lu, Z.; Yin, Y. *Chem. Soc. Rev.* **2012**, *41*, 6874. (e) Talapin, D. V.; Lee, J. S.; Kovalenko, M. V.; Shevchenko, E. V. *Chem. Rev.* **2010**, *110*, 389.

(5) (a) Black, C. T.; Murray, C. B.; Sandstrom, R. L.; Sun, S. H. *Science* **2000**, *290*, 1131. (b) Courty, A.; Mermet, A.; Albouy, P. A.; Duval, E.; Pileni, M. P. *Nat. Mater.* **2005**, *4*, 395. (c) Talapin, D. V.; Murray, C. B. *Science* **2005**, *310*, 86. (d) Yamada, Y.; Tsung, C. K.; Huang, W.; Huo, Z. Y.; Habas, S. E.; Soejima, T.; Aliaga, C. E.; Somorjai, G. A.; Yang, P. D. *Nat. Chem.* **2011**, *3*, 372. (e) Collier, C. P.; Saykally, R. J.; Shiang, J. J.; Henrichs, S. E.; Heath, J. R. *Science* **1997**, *277*, 1978. (f) Sun, S. H.; Murray, C. B.; Weller, D.; Folks, L.; Moser, A. *Science* **2000**, *287*, 1989. (g) Dong, A. G.; Chen, J.; Vora, P. M.; Kikkawa, J. M.; Murray, C. B. *Nature* **2010**, *466*, 474.

(6) (a) Rycenga, M.; McLellan, J. M.; Xia, Y. N. *Adv. Mater.* **2008**, *20*, 2416. (b) Miszta, K.; de Graaf, J.; Bertoni, G.; Dorfs, D.; Brescia, R.; Marras, S.; Ceseracciu, L.; Cingolani, R.; van Roij, R.; Dijkstra, M.; Manna, L. *Nat. Mater.* **2011**, *10*, 872. (c) Jones, M. R.; Macfarlane, R. J.; Lee, B.; Zhang, J. A.; Young, K. L.; Senesi, A. J.; Mirkin, C. A. *Nat. Mater.* **2010**, *9*, 913. (d) DeVries, G. A.; Brunnbauer, M.; Hu, Y.; Jackson, A. M.; Long, B.; Neltner, B. T.; Uzun, O.; Wunsch, B. H.; Stellacci, F. *Science* **2007**, *315*, 358.

(7) Wang, T.; J.; Lynch, J.; Chen, O.; Wang, Z. L.; Wang, X.; LaMontagne, D.; Wu, H.; Wang, Z. W.; Cao, Y. C. *Science* **2012**, *338*, 358.

(8) (a) Zhuang, J.; Wu, H.; Yang, Y.; Cao, Y. C. *J. Am. Chem. Soc.* **2007**, *129*, 14166. (b) Zhuang, J.; Wu, H.; Yang, Y.; Cao, Y. C. *Angew. Chem., Int. Ed.* **2008**, *47*, 2208. (c) Zhuang, J.; Shaller, A. D.; Lynch, J.; Wu, H.; Chen, O.; Li, A. D. Q.; Cao, Y. C. *J. Am. Chem. Soc.* **2009**, *131*, 6084. (d) Wang, T.; Wang, X.; LaMontagne, D.; Wang, Z. L.; Wang, Z. W.; Cao, Y. C. *J. Am. Chem. Soc.* **2012**, *134*, 18225.

(9) (a) Carbone, L.; Nobile, C.; De Giorgi, M.; Sala, F. D.; Morello, G.; Pompa, P.; Hytch, M.; Snoeck, E.; Fiore, A.; Franchini, I. R.; Nadasan, M.; Silvestre, A. F.; Chiodo, L.; Kudera, S.; Cingolani, R.; Krahne, R.; Manna, L. *Nano Lett.* **2007**, *7*, 2942. (b) Talapin, D. V.; Nelson, J. H.; Shevchenko, E. V.; Aloni, S.; Sadtler, B.; Alivisatos, A. P. *Nano Lett.* **2007**, *7*, 2951.

(10) Nagaoka, Y.; Wang, T.; Lynch, J.; LaMontagne, D.; Cao, Y. C. *Small* **2012**, *8*, 843.

(11) Einstein, A. *Ann. Phys. Berlin* **1905**, *17*, 549.

(12) Xia, Y. N.; Yin, Y. D.; Lu, Y.; McLellan, J. *Adv. Funct. Mater.* **2003**, *13*, 907.

(13) (a) Sitt, A.; Salant, A.; Menagen, G.; Banin, U. *Nano Lett.* **2011**, *11*, 2054. (b) Talapin, D. V.; Koeppe, R.; Gotzinger, S.; Kornowski, A.; Lupton, J. M.; Rogach, A. L.; Benson, O.; Feldmann, J.; Weller, H. *Nano Lett.* **2003**, *3*, 1677.

(14) (a) Wang, S. Y.; Querner, C.; Dadosh, T.; Crouch, C. H.; Novikov, D. S.; Drndic, M. *Nat. Commun.* **2011**, *2*, 364. (b) Wang, J. F.; Gudiksen, M. S.; Duan, X. F.; Cui, Y.; Lieber, C. M. *Science* **2001**, *293*, 1455.

(15) Yeh, P.; Gu, C. *Optics of Liquid Crystal Displays*; Wiley: Hoboken, NJ, 2010.